

Ba Adsorption on the Stoichiometric and Defective TiO₂ (110) Surface from First-Principles Calculations

M. A. San Miguel,* J. Oviedo, and J. F. Sanz

Departamento de Química Física, Facultad de Química, Universidad de Sevilla, c/ Profesor García González, 2, 41012 Sevilla, Spain

Received: June 15, 2006; In Final Form: August 3, 2006

A theoretical study on Ba adsorption on the rutile TiO₂ (110) surface has been carried out by means of plane-wave, plane augmented waves potential, density functional theory calculations. A model consisting on a (4 × 1) unit cell, which corresponds to coverage of 0.125 monolayer (ML), has been used and several potential adsorption sites on the stoichiometric surface have been tried. It has been found that the most stable site is with the Ba atom in a position where it is bound to two bridging oxygen atoms and an in-plane oxygen atom forming equivalent bonds (OB site). The adsorption energy is 0.71 eV referred to the formation of Ba bulk and is about 0.3 eV more stable than other adsorption sites. The Ba–surface interaction produces some surface relaxation in all cases. The OB site is stable at moderate temperatures; however, after extensive molecular dynamic calculations it is found that atoms diffuse on the surface by means of a jumping mechanism among several stable positions. The presence of bridging oxygen vacancies does not alter significantly this picture since the adsorption close to defects is not energetically favorable and the atoms tend to move away from vacancies. A strong covalent character has been found in the nature of the bonding, which contrasts with previous suggestions of the existence of Ba²⁺ species on the surface. When the coverage is increased to 0.25 ML by adding a Ba atom to the supercell, there is a significant repulsion between Ba atoms that move away from each other to occupy OB sites. Thus, the adsorption energy values per atom diminish. For the stoichiometric surface two equivalent adsorption patterns are found, whereas only one is found for the defective surface.

Introduction

There has been an increasing effort in studying transition metal oxides during the past decade because of their broad technological applicability.¹ Among these systems, titanium dioxide has been one of the most investigated compounds. There are two important structures of TiO₂, anatase and rutile.² Rutile has been extensively characterized; among the different low-index surfaces, the (110) is the most stable and also the most studied.² This surface is readily and reproducibly prepared, so it has been considered a prototype of metal oxide surface.¹ Its structure can be described as formed by neutral layers. Each layer is made of three planes of composition, O–Ti₂O₂–O. In the surface, there are two kinds of titanium atoms, 5-fold and 6-fold coordinated, forming alternating rows. All oxygen atoms are 3-fold coordinated as in the bulk except those ones in the outermost plane called bridging atoms, which lose one bond when the upper layer is removed.

Alkali and alkaline earth metals are known to behave as reaction modifiers on a variety of substrates, including metal oxides. Several studies have been carried out on alkali metal adsorption on the TiO₂ (110) surfaces.¹ For example, after adsorption of Na or K there are important changes in the electronic structure of TiO₂, via oxidation of the adsorbed alkali and reduction of the Ti atoms in the substrate.³ There have been several proposals about where the alkali metals are located and which models describe better their distribution on the surface depending on the coverage.⁴

On the other hand, studies of adsorption of alkaline earth metals (Ca, Sr, Ba) on the same substrate are still scarce.^{5–7} Since their electronic structure differs from that of alkali metals, studies on the charge-transfer process from alkaline earth metals to substrate and its relation to catalytic reactivity are very interesting.

In a previous photoemission experimental study, there was evidence of charge transfer from adsorbed Ba atoms to titanium on the surface.⁵ It was suggested that some Ti atoms were reduced to a Ti³⁺ state, which corresponds to a peak in the valence band spectra. When the Ba coverage increases over the monolayer regime, there is evidence of metallic Ba states on the surface. There has also been some work on Ca adsorption.^{6,7} In this case, there is still controversy about whether the calcium is present as Ca²⁺ or not.

To the best of our knowledge, there is no previous theoretical work on this system. Here we present a density functional study of Ba adsorption on the stoichiometric and defective TiO₂ (110) surface. On the stoichiometric surface, we have scanned several adsorption sites and analyzed the electronic structure of the most stable structures. The existence of oxygen vacancies on this surface is well-known. Specifically, the bridging oxygen atoms are missing up to 10%.¹ The presence of vacancies changes the surface electronic structure and therefore it has also been considered how this fact could affect the adsorption process.

Traditionally, computer studies have been carried out under static conditions, that is, geometry optimizations that formally correspond to calculations at 0 K. However, it is clear that temperature plays an important role in surface processes. The

* Corresponding author: e-mail smiguel@us.es.

steady growth of computational resources makes it feasible to include temperature effects even for moderately large systems. Therefore, molecular dynamic (MD) calculations have been performed at several temperatures for some representative situations. The paper is organized as follows. The next section describes the technical details about the calculations. This is followed by a section where the main results are discussed, starting from the stoichiometric to the defective surface and from static to dynamic calculations, respectively. In addition, by increasing Ba coverage, the role of Ba–Ba interaction is analyzed. Finally, some conclusions are drawn.

Technical Details

In the present work, the implementation of density functional theory (DFT) has been used with plane waves and the PAW (plane augmented waves) potentials.^{8–10} We use the generalized gradient approximation (GGA) for the exchange–correlation energy, which seems to describe better the formation and creation of bonds on surfaces.¹¹ In particular, we use the GGA of Perdew et al.^{12,13}

The calculations were performed with the VASP (Vienna ab initio simulation package) code.^{14–16} This is a particularly efficient and stable code, which searches for the self-consistent ground state by use of residual minimization and charge mixing. In this code, the forces on the atoms are automatically calculated, and relaxation of all atoms in the system to their equilibrium position is also automatic.

In this kind of calculation, we must decide which states are treated as core states and which as valence states. For oxygen, the core consists only of 1s states, whereas for Ti, up to and including the 3p shells are frozen and the reference state for the potential generation is s¹d³. For barium, 10 electrons (5s²–5p⁶6s²) are described as valence states. The PAW potentials included in the VASP package were used.^{10,17}

The surface was represented by means of a four-layer slab made of (4 × 1) unit cells. To study defective surfaces, one bridging oxygen has been removed from the supercell and thus the system represented a surface with a 25% oxygen vacancy concentration. An energy cutoff of 400 eV was set, and the calculations were performed at the Γ point of the Brillouin zone. The optimized lattice parameters are $a = 4.616$ Å, $c = 2.974$ Å, and $u = 0.304$ and have been used for the (110) surface throughout the present work and maintained fixed during the atomic positions relaxation. Full convergence tests and technical details can be found in a previous work.¹⁸ The model with one Ba atom per supercell corresponds to a surface coverage of 0.125 ML, whereas for the coadsorption studies is increased to 0.25 ML.

To analyze dynamical effects, MD calculations were performed in the canonical ensemble at 100 and 300 K. The time step was 3 fs and a typical simulation spanned about 10 ps.

Results and Discussions

(a) Stoichiometric Surface. Ba adsorption has been studied on several adsorption sites on the stoichiometric surface. There is very little known about which is the preferred site for this atom. This is a general situation for other alkaline earth metals. For instance, in a previous work on Ca adsorption, several alternatives have been proposed.⁶ Figure 1 shows a top-view surface where several adsorption sites are indicated. Two of them consist of adsorption over bridging oxygen atoms: one site is on top of a single bridging atom (TB) and the other site is between two of them (BB). We also tried adsorption over a 5-fold Ti (TiP) and finally on positions with the barium atom

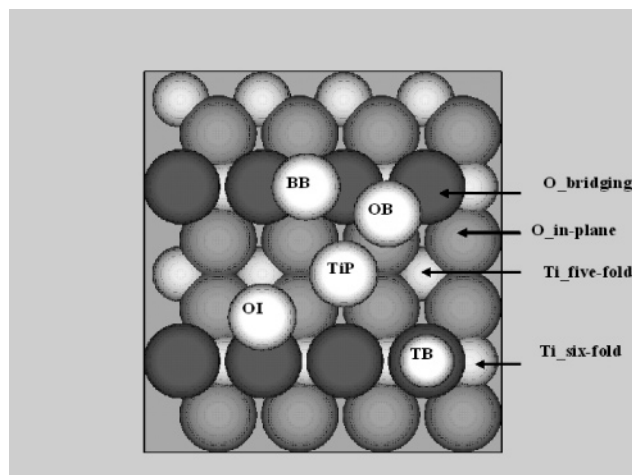


Figure 1. Top view of the TiO₂ (110) surface. Some representative atom types and the five adsorption sites reported in this work are labeled in the figure.

among three oxygens. One site is between two bridging oxygen and one in-plane oxygen atom (OB), and the other site is between one bridging oxygen and two in-plane oxygen atoms (OI).

Among these adsorption sites, only three were minima in the potential energy surface. In BB, OB, and OI sites, the Ba atom binds to one or two bridging oxygens. The other two sites, TiP and TB, were found to be unstable and the optimization process moved the Ba atom toward OI and BB sites, respectively.

Figure 2 shows the optimized geometries. In the BB situation the Ba atom is bound to two equivalent bridging oxygen atoms, whereas in OB and OI sites the Ba is positioned among three oxygen atoms. Table 1 shows the bond distances and some representative distance relaxations. In OB and OI sites, the Ba atom lies at a shorter distance from the surface and relaxations are more noticeable. Since the Ba stays at a certain distance above the surface, the oxygen atoms directly bound to Ba tend to move upward. This displacement is especially large for in-plane atoms that have to move in order to form bonds with the adsorbed metal. The movements are as large as 0.36 Å for OI and 0.26 Å for OB and can be seen clearly in Figure 2b,c. Titanium atoms under the bridging oxygen row also move, and the Ti–O bridging bond distances are stretched.

The adsorption energy, defined as the energy required to remove the barium from the surface and to create metallic barium in the bulk, has been computed as

$$E_{\text{ads}} = E_{\text{Ba-TiO}_2}(\text{surf}) - E_{\text{TiO}_2}(\text{surf}) - nE_{\text{Ba}}(\text{bulk}) \quad (1)$$

where $E_{\text{Ba-TiO}_2}$ and E_{TiO_2} are the total energies of the Ba-adsorbed and bare surface slabs, respectively; n is the number of adsorbed Ba atoms; and E_{Ba} is the total energy per atom of the metallic barium bulk. This energy was chosen as the reference for the barium atom since it is the most stable state. We should emphasize that in order to get meaningful results we have carried out calculations of every term in the above equation under exactly the same technical conditions in order to get an effective cancellation of errors.

From an energetic point of view, the Ba atom is more stable when it is 3-fold coordinated and thus the OB and OI sites are more stable than the BB site. Between them, the OB site is the most stable by 0.28 eV. This is essentially linked to the fact that the bond distances to the oxygen atoms are more balanced in the OB situation (2.45 and 2.55 Å for OB vs 2.37 and 2.63 Å for OI).

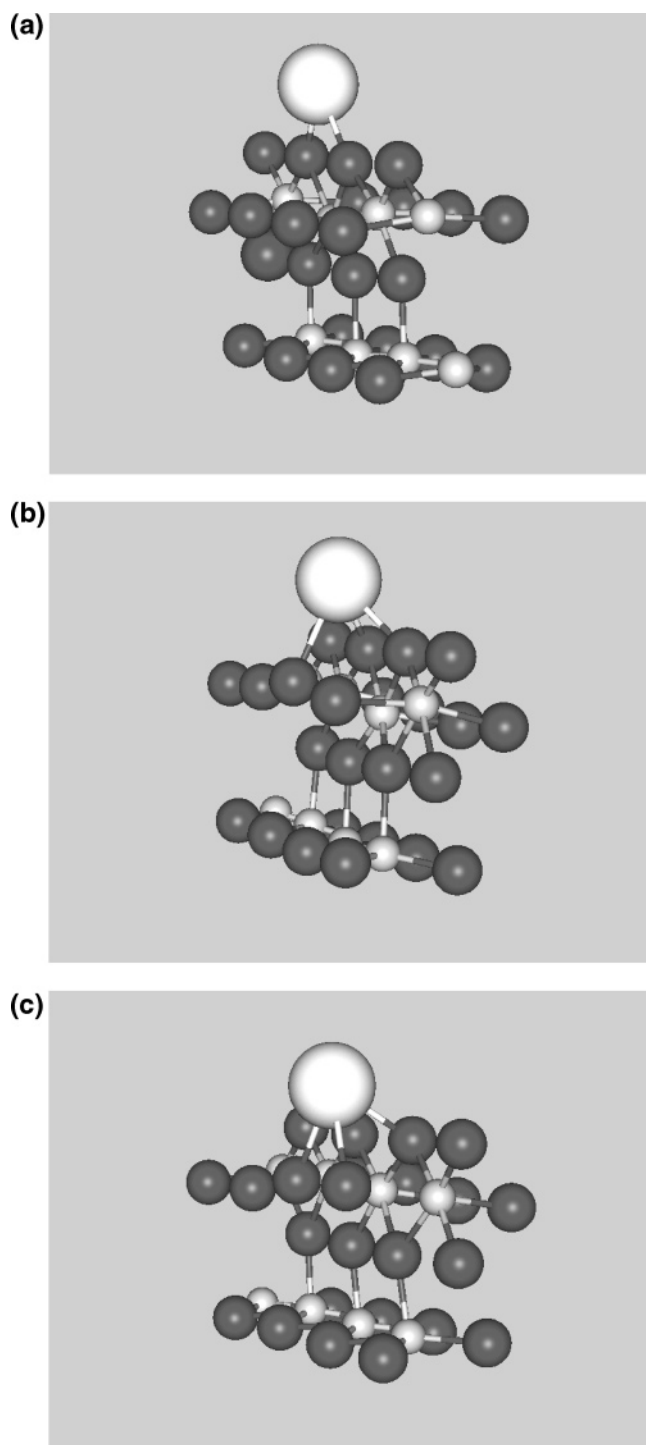


Figure 2. Optimized geometries for several cases discussed within the text for the stoichiometric surface: (a) BB; (b) OB; (c) OI. Only a portion of the surface is shown. Oxygen is represented by dark spheres, whereas small and large light spheres represent titanium and barium, respectively.

To get a deeper insight into the adsorption mechanism, the electronic structure was analyzed. The density of states does not show any feature clearly assignable to Ba atom but the one corresponding to the 5p states, which arises well below the valence band. The Ba s and d states appear mixed in both the valence and conduction bands. As expected from the reduction process upon Ba adsorption, the Fermi level is moved from the top of the valence band in the bare stoichiometric surface to the bottom of the conduction band, indicating a change in the electron conduction properties.

TABLE 1: Adsorption Energies and Some Optimized Geometrical Parameters for the Stable Adsorption Sites on the Stoichiometric TiO₂(110) Surface^a

sites	E_{ads} (eV)	Ba–O _{br} (Å)	Ba–O _{in} (Å)	O _{in} (Δz) (Å)	Ti (Δz) (Å)
BB	−0.38	2.36	3.59	0	−0.37
OB	−0.71	2.45	2.55	0.26	−0.36
OI	−0.43	2.37	2.63	0.36	−0.19

^a O_{br} and O_{in} mean bridging and in-plane oxygen, respectively. Ti is the 6-fold coordinated titanium bound to the bridging oxygen atoms. The z axis is perpendicular to the surface, and displacements are positive when the atoms move outward the surface.

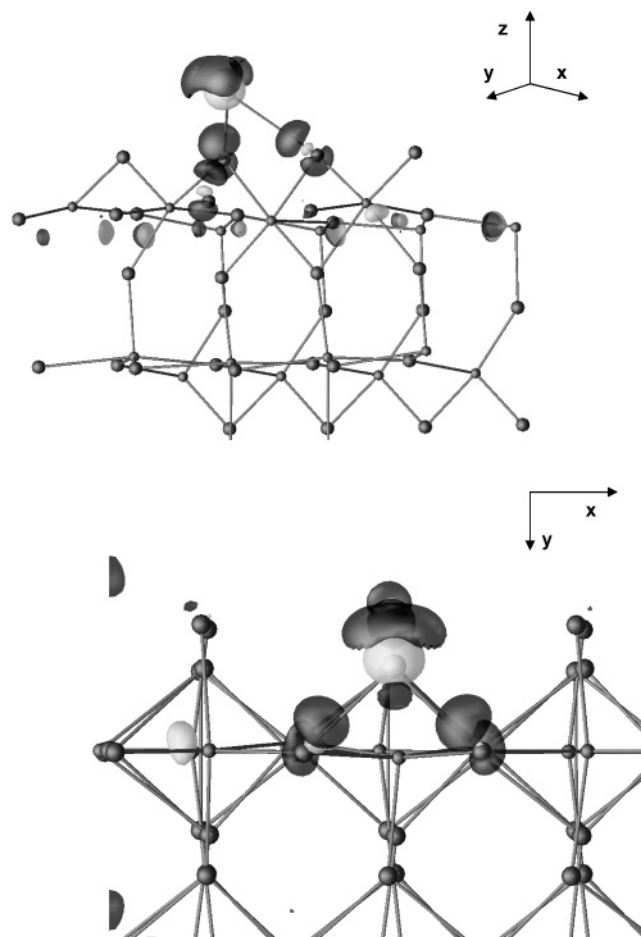


Figure 3. Charge density difference maps for the OB case. All atoms are represented by small spheres. Grey and dark gray show negative and positive charge transfer, respectively. (Upper panel) Side view; (lower panel) top view.

Analysis of the differences in charge density is particularly meaningful. They are computed through the formula

$$\Delta\rho = \rho(\{\text{system}\}) - \rho(\{\text{surf}\}) - \rho(\{\text{Ba}\})$$

where the charge densities of the surface and the Ba atom are calculated on the geometries obtained from the optimization of the whole system. In this way, $\Delta\rho$ reflects how the charge density is localized in space after the adsorption process as compared to the isolated fragments. Thus, positive values would correspond to density gain and negative values to density loss.

Figure 3 shows $\Delta\rho$ as surfaces of values of $\Delta\rho = +0.04e$ (dark gray) and $\Delta\rho = -0.04e$ (light gray) for the OB site where the Ba atom is located among three oxygens forming equivalents bonds. It is clear that there is some charge transfer from the Ba atom to the surface oxygen atoms. It is not possible for us to quantify the charge transfer but a bond directionality is clear,

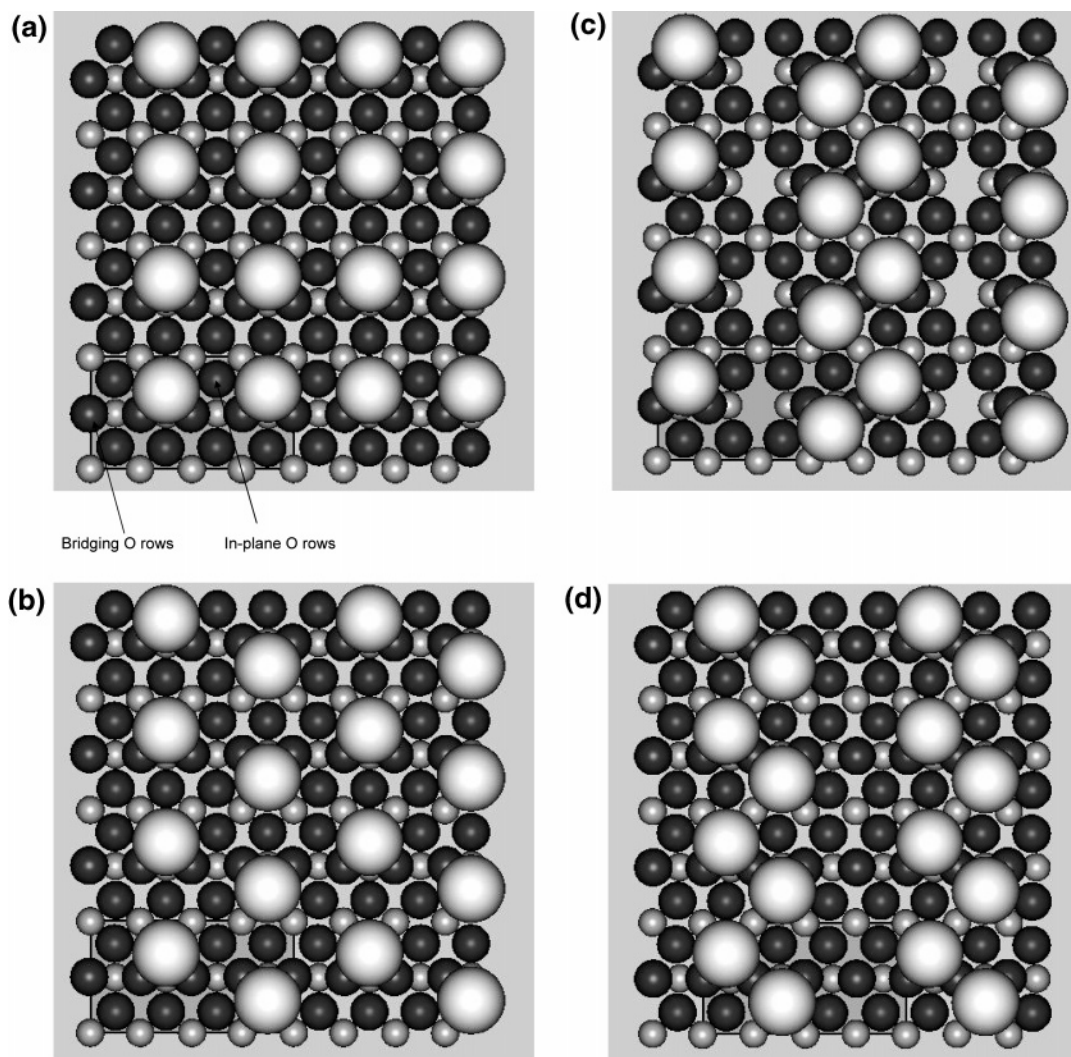


Figure 4. Different coadsorption surface patterns ($\theta = 0.250$ ML) for the stoichiometric surface (a) SS, (b) OS, and (d) OSC models and for the defective surface (c) OSC model. Ba atoms are represented by the largest spheres, Ti atoms are represented by the smallest spheres, and O atoms are shown by the medium ones (dark gray). A box indicates the supercell in each model, and the bridging and in-plane O rows are pointed out in panel a.

TABLE 2: Adsorption Energies^a for One Ba Atom and Two Ba Atoms on a (4 × 1) Surface Supercell for Three Different Models

	E_{ads} (eV)				$E_{\text{ads-2}}$ (eV)		
	1Ba	OS	SS	OSC	OS	SS	OSC
STOI	-0.71	-0.41	-0.40	-0.17	+0.30	+0.31	+0.54
VAC	-0.18			+0.23			+0.41

^a Calculated as indicated in the text.

which indicates a significant covalent character. This is in contrast to the previous suggestion that Ba is in a +2 oxidation state.⁵

To introduce temperature effects, MD calculations were performed. Two regimes were studied: 100 and 300 K. At low temperature, Ba atoms have enough kinetic energy to move from their initial adsorption sites to the most stable OB site. The atom is then confined here even for long simulations. With increasing temperature, the Ba atom eventually gets enough energy to move from one OB site to the contiguous OB site in the front bridging O row, which essentially means diffusion along the [001] direction. Our simulations lasting for 7.5 ps only showed one of these events.

No jumps from an OB site to another one on the other side of the bridging O row were observed, that is, diffusion along

the $[1\bar{1}0]$ direction. The transition barrier for this event can be roughly estimated as the energy difference between OB and BB sites (i.e., 0.33 eV). Since the time spanned by MD simulations is relatively short compared to experiments, it is not straightforward to observe processes where an energy barrier has to be surmounted such as this case. From our simulations we do not exclude diffusion along the $[1\bar{1}0]$ direction, but it seems easier by far for Ba atoms to diffuse parallel to bridging O rows along the [001] direction, although the jump frequency is still very low at 300 K.

(b) Defective Surface. For the defective surface all the adsorption sites described above were studied, and additionally others related to the presence of the oxygen vacancy were included, such as on top of the defect or an OB site adjacent to the vacancy.

The geometry optimizations indicated that the most stable adsorption site is an OB site far from the vacancy, although the adsorption energy value decreases from 0.71 eV in the stoichiometric surface to 0.18 eV. The magnitude of the relaxation in the surface for the OB site is similar to the corresponding value for the stoichiometric surface. Thus, the in-plane oxygen bound to the Ba atom moves upward and the hexa-fold Ti atom moves downward by 0.3 Å.

MD simulations at low temperature showed how Ba atoms diffuse from the vacancy site to nearby OB sites. It seems that

Ba atoms adsorbed on a defective TiO₂(110) surface would move away from the vacancies. Therefore, the surface reduction by the formation of vacancies deactivates the system and Ba adsorption becomes less favorable.

(c) Coadsorption. To study the effect of increasing the Ba coverage, an additional Ba atom was introduced in the supercell. Here we follow the coverage definition that 0.5 monolayer (ML) corresponds to the deposition of as many metal atoms as penta-fold Ti atoms in the unit cell;^{19,20} thus the coverage goes from 0.125 to 0.250 ML.

As discussed previously, the preferential adsorption site for Ba is an OB site. The addition of an extra metal atom on the surface can be done on a position at the same side of the bridging oxygen row (SS) or at the opposite side (OS). Both possibilities have been considered, and MD simulations were performed from several starting configurations at 100 K.

It is clear from the MD results that the metal atoms on the surface compete to occupy OB sites and to be as far away as possible from each other. Simulations for the stoichiometric surface lead to two different adsorption patterns that are shown in Figure 4. In the SS model (Figure 4a) the Ba atoms occupy two OB sites at the same side of the bridging oxygen row, leaving free one OB site between occupied sites in order to minimize the Ba–Ba repulsions. In a similar way, in the OS model (Figure 4b) the occupied OB sites are at opposite sides of the bridging O row, leaving one free site.

For the defective surface, the most stable configuration is with the Ba atoms placed in OB sites as in the OS model, but the presence of an oxygen vacancy restricts them to be in contiguous positions. This model has been named as OSC (Figure 4c).

The final geometries for all these models were optimized and the adsorption energies for two atoms were obtained in the traditional way from eq 1, where n is 2. The calculated values are reported in Table 2 along with the adsorption energies for one Ba atom on the bare surface. It can be seen that the total adsorption energy (E_{ads}) decreases appreciably when a second metal atom is added and becomes positive, that is, the adsorption is not favorable, for the OSC model in the defective surface. For comparative purposes, the OSC model was also considered for the stoichiometric surface (Figure 4d) although it is less stable than the SS and OS models. The similar adsorption energy values corresponding to the OS and SS models indicate that both patterns would be found indistinguishably for a stoichiometric surface, whereas the OSC would be the only one present for defective surfaces.

To analyze these results more deeply, the contribution to the adsorption energy due to the addition of the second Ba atom (when one Ba atom is already adsorbed) has been computed as

$$E_{\text{ads}-2} = E_{2\text{Ba-TiO}_2}(\text{surf}) - E_{\text{Ba-TiO}_2}(\text{surf}) - E_{\text{Ba}}(\text{bulk}) \quad (2)$$

On doing this, $E_{\text{ads}-2}$ reflects the contribution of the second Ba atom to the whole process. All the values are positive, which indicates that the addition introduces repulsive forces due to Ba–Ba interactions more intense than the attractive interactions caused by the formation of Ba–O bonds.

Conclusions

From this study several conclusions can be drawn. For the stoichiometric surface, several adsorption sites have been considered, although only three are actually stable. The most stable one corresponds to adsorption of Ba on a position where it is bound to two bridging oxygens and one in-plane oxygen, forming equivalent bonds. This site is about 0.3 eV more stable than the others. There is a considerable Ba–surface interaction. This also produces a noticeable surface relaxation, especially in the OB site. From the analysis of differences in charge density some charge transfer is found from the Ba atom to the surface, but essentially the bond has a covalent character. We do not see evidence to support the idea that the Ba is in a +2 oxidation state.

A defective surface has been considered by the presence of a bridging oxygen vacancy in the (4 × 1) surface supercell. The net effect is that the Ba atoms move away from the vacancies, since the adsorption energy is smaller, and occupy OB sites. MD simulations further confirm this.

The effect of adding an extra Ba atom in the supercell has also been studied from MD simulations and geometry optimizations. The repulsive forces cause Ba atoms to be as far as possible from each other and to occupy OB sites. For the stoichiometric surface, two equivalent adsorption patterns were found, named SS and OS, whereas for the defective surface only the OSC model was observed. The bond nature in all these cases is the same as that found for one Ba atom, although the net adsorption energies decrease due to the Ba–Ba repulsive interactions.

Acknowledgment. This work was funded by the Spanish Ministerio de Educación y Ciencia, Project MAT2005-01872.

References and Notes

- (1) Diebold, U. *Surf. Sci. Rep.* **2003**, *48*, 53.
- (2) Henrich, V. E.; Cox, P. A. In *The Surface Science of Metal Oxides*; Cambridge University Press: Cambridge, U.K., 1996.
- (3) Calzado, C. J.; San Miguel, M. A.; Sanz, J. F. *J. Phys. Chem. B* **1999**, *103*, 480.
- (4) San Miguel, M. A.; Calzado, C. J.; Sanz, J. F. *J. Phys. Chem. B* **2001**, *105*, 1794 and references therein.
- (5) Li, Z.; Hoffmann Jørgensen, J.; Møller, P. J.; Sami, M.; Granozzi, G. *Appl. Surf. Sci.* **1999**, *142*, 135.
- (6) Bikondoa, O.; Pang, C. L.; Muryn, C. A.; Daniels, B. G.; Ferrero, S.; Michelangeli, E.; Thornton, G. *J. Phys. Chem. B* **2004**, *108*, 16768.
- (7) Zhang, L. P.; Li, M.; Diebold, U. *Surf. Sci.* **1998**, *412/413*, 242.
- (8) Payne, M. C.; Teter, M. P.; Allan, D. C.; Arias, T. A.; Joannopoulos, J. D. *Rev. Mod. Phys.* **1992**, *64*, 1045.
- (9) Blöchl, P. E. *Phys. Rev. B* **1994**, *50*, 17953.
- (10) Kresse, G.; Joubert, J. *Phys. Rev. B* **1999**, *59*, 1758.
- (11) Hu, P.; King, D. A.; Crampin, S.; Lee, M.-H.; Payne, M. C. *Chem. Phys. Lett.* **1994**, *230*, 501.
- (12) Perdew, J. P. In *Electronic Structure in Solids '91*; Ziesche, P., Eschrig, H., Eds.; Akademie Verlag: Berlin, 1991.
- (13) Perdew, J. P.; Chevary, J. A.; Vosko, S. H.; Jackson, K. A.; Pederson, M. R.; Singh, D. J.; Fiolhais, C. *Phys. Rev. B* **1992**, *46*, 6671.
- (14) Kresse, G.; Hafner, J. *Phys. Rev. B* **1993**, *47*, 558.
- (15) Kresse, G.; Furthmüller, J. *Comput. Mater. Sci.* **1996**, *6*, 15.
- (16) Kresse, G.; Furthmüller, J. *Phys. Rev. B* **1996**, *54*, 11169.
- (17) Vanderbilt, D. *Phys. Rev. B* **1990**, *41*, 7892.
- (18) Oviedo, J.; San Miguel, M. A.; Sanz, J. F. *J. Chem. Phys.* **2004**, *121*, 7427.
- (19) Onishi, H.; Aruga, T.; Egawa, C.; Iwasawa, Y. *Surf. Sci.* **1988**, *199*, 54.
- (20) San Miguel, M. A.; Calzado, C. J.; Sanz, J. F. *Surf. Sci.* **1998**, *409*, 92.